# Exocytosis of Vacuolar Apical Compartment (VAC): A Cell-Cell Contact Controlled Mechanism for the Establishment of the Apical Plasma Membrane Domain in Epithelial Cells

**Dora E. Vega-Salas, Pedro J. I. Salas, and Enrique Rodriguez-Boulan**

Department of Cell Biology and Anatomy, Cornell University Medical College, New York 10021

*Abstract.* The vacuolar apical compartment (VAC) is an organelle found in Madin-Darby canine kidney (MDCK) cells with incomplete intercellular contacts by incubation in 5 μM $Ca^{++}$ and in cells without contacts (single cells in subconfluent culture); characteristically, it displays apical biochemical markers and microvilli and excludes basolateral markers (Vega-Salas, D. E., P. J. I. Salas, and E. Rodriguez-Boulan. 1987. *J. Cell Biol.* 104:1249–1259). The apical surface of cells kept under these culture conditions is immature, with reduced numbers of microvilli and decreased levels of an apical biochemical marker (184 kD), which is, however, still highly polarized (Vega-Salas, D. E., P. J. I. Salas, D. Gundersen, and E. Rodriguez-Boulan. 1987. *J. Cell Biol.* 104:905–916). We describe here the morphological stages of VAC exocytosis which ultimately lead to the establishment of a differentiated apical domain. Addition of 1.8 mM $Ca^{++}$ to monolayers developed in 5 μM $Ca^{++}$ causes the rapid (20–40 min) fusion of VACs with the plasma membrane and their accessibility to external antibodies, as demonstrated by immunofluorescence, immunoperoxidase EM, and RIA with antibodies against the 184-kD apical plasma membrane marker. Exocytosis occurs towards areas of cell-cell contact in the developing lateral surface where they form intercellular pockets; fusion images are always observed immediately adjacent to the incomplete junctional bands detected by the ZO-1 antibody (Stevenson, B. R., J. D. Siliciano, M. S. Mooseker, and D. A. Goodenough. 1986. *J. Cell Biol.* 103:755–766). Blocks of newly incorporated VAC microvilli and 184-kD protein progressively move from intercellular ("primitive" lateral) spaces towards the microvilli-poor free cell surface. The definitive lateral domain is sealed behind these blocks by the growing tight junctional fence. These results demonstrate a fundamental role of cell-cell contact-mediated VAC exocytosis in the establishment of epithelial surface polarity. Because isolated stages (intercellular pockets) of the stereotyped sequence of events triggered by the establishment of intercellular contacts in MDCK cells have been reported during normal differentiation of intestine epithelium (Colony, P. C., and M. R. Neutra. 1983. *Dev. Biol.* 97:349–363), we speculate that the mechanism we describe here plays an important role in the establishment of epithelial cell polarity in vivo.

THE asymmetric distribution of plasma membrane components into apical and basolateral domains (polarity) is essential for the vectorial functions of differentiated epithelial tissues (51, 55). Epithelial cells in tissue culture are useful models to study the mechanisms responsible for polarization and differentiation (4, 9, 24, 25, 27, 65).

We have recently described a 184-kD apical plasma membrane antigen of Madin-Darby canine kidney (MDCK) cells which is highly polarized in confluent monolayers. MDCK cells prevented from forming complete cell-cell contacts by incubation in low calcium DME (LC; ~5 μM $Ca^{++}$), have reduced levels of this antigen on the surface (38%), although it is equally well polarized (15-fold more concentrated in the apical than in the basolateral domain) into a "primitive" (biochemically mixed) apical domain (Figs. 4 *C* and 5 *B* in reference 65) that also contains basolateral markers (i.e., a 63-kD membrane protein). The remaining portion of the 184-kD protein (62%) is found in an intracellular vacuolar structure: the vacuolar apical compartment (VAC),[1] an organelle only seen in cells which have not yet developed intercellular contacts (such as single cells) and in monolayers prevented from developing complete cell-cell contacts by incubation in LC (~5 μM; reference 20). Indeed, cells kept in LC have fewer microvilli on their surface (but accumulate them in VACs)

Dora E. Vega-Salas' and Pedro J. I. Salas' present address is Instituto de Investigaciones Bioquimícas, Fundación Campomar, 1405 Buenos Aires, Argentina.

1. *Abbreviations used in this paper*: LC, low calcium DME; NC, normal calcium DME; PFA, paraformaldehyde; VAC, vacuolar apical compartment.

and a much smaller average lateral domain than normal monolayers (16% of the surface area vs. 58% of the total cell surface area in normal calcium DME [NC], NC = 1.8 mM $Ca^{++}$). Influenza virus hemagglutinin, an apical marker in infected MDCK cells (51), is targeted both to VACs and to the free apical surface. On the other hand, basolateral markers (a 63-kD basolateral cellular protein and vesicular stomatitis virus G glycoprotein) are detected at similar concentrations on the free and attached surfaces of cells kept in LC but are excluded from VACs (66).

VAC-like structures have been described in several epithelia (19, 46, 48, 49, 62; see reference 47 for a review), tumors of epithelial lineage (7, 30–32, 60, 61, 63), and even in lower vertebrates (1, 33) on the basis of a purely ultrastructural criterion: intracellular lumina with microvilli and positive stain to polysaccharides (12). The wide distribution of these structures suggests an important and poorly understood function in the biogenesis of epithelia.

The concentration of apical plasma membrane components in VACs and initial kinetic observations (66) suggest a precursor role for VACs in the formation of the apical surface of epithelial cells. The experiments in this report describe kinetically and structurally the early events in the exocytosis of VAC and the subsequent redistribution of the newly inserted apical components to their final localization in the apical pole. Cell–cell contacts were found to play an important role, not only in the control of VAC exocytosis, but also in the spatial organization of the process.

## Materials and Methods

### Cell Culture

MDCK strain II (38) between passages 58 and 75 were cultured in 75-$cm^2$ tissue culture flasks (Falcon Labware, Oxnard, CA), at 37°C, 5% $CO_2$ in DME containing 1.8 mM Ca (NC; Gibco Laboratories, Grand Island, NY), supplemented with 10% horse serum (HyClone Laboratories, Logan, UT). The cells were dissociated weekly by treatment with 0.25% trypsin/0.2 mM EDTA. For experiments, cells were plated in serum-free DME after dissociation and, in some cases, changed to LC (spinner-MEM, containing 1–5 μM calcium, 10 mM phosphate; Gibco Laboratories) 90 min after plating (66).

### Antibodies, Radioimmunoassay, and Immunofluorescence

The preparation and characterization of the S2/2G1 mAb against a 184-kD MDCK apical plasma membrane protein have been described elsewhere (65, 66). The rat mAb against ZO-1, a 225-kD tight junctional protein was obtained and characterized by Stevenson et al. (57).

Fab fragments were prepared from the S2/2G1 mAb as by Edidin and Wei (17). Briefly, the Ig was purified by precipitation with 50% $(NH_4)_2SO_4$ followed by DEAE-cellulose ion exchange chromatography and dialyzed against 0.15 M NaCl, 0.001 M $Na_2$-EDTA, 0.1 M potassium phosphate, pH 8.0. Then, 5 mg Ig (2 ml) was incubated with 40 U of 2× crystallized papain (Sigma Chemical Co., St. Louis, MO) previously activated for 15 min at room temperature in 0.1 M sodium acetate, 0.01 M cysteine, and 0.001 M EDTA buffer. The digestion was stopped by adding solid iodoacetamide up to a final concentration of 0.05 M. Undigested Ig and Fab fragments were separated by chromatography on a Sephadex G-100 column (1.5 × 50 cm). Fractions corresponding to the second peak, which contained most of Fab, as determined by SDS-PAGE were collected and rechromatographed once to eliminate all undigested antibody. The Fab fragment was tested by indirect immunofluorescence on formaldehyde-fixed MDCK monolayers, concentrated against solid polyvinyl pyrrolidone ($M_r$ 40,000; Sigma Chemical Co.) and stored at −20°C.

For RIA and immunofluorescence, the cells were fixed in 2% formaldehyde in PBS, freshly prepared from paraformaldehyde (PFA) at 4°C, or in 96% methanol at −20°C when ZO-1 antibody was used. Cells were sequentially incubated with 50 mM $NH_4Cl$, 1% BSA, and 50 μg/ml of preimmune IgG from the same species as the second antibodies (usually goat) in PBS. For double immunofluorescence, BSA was avoided and the cells were sequentially incubated with one first antibody, its corresponding second antibody, and then, similarly, for the other antigen. For colocalization of mAb Fab fragments and whole mAb IgG, affinity-purified Fab or Fc-specific second antibodies (Jackson Immuno Research Laboratories, Inc., West Grove, PA) were used. After five washes in PBS, the cells were mounted on a drop of 20% polyvinyl alcohol (Vinol; Air Products and Chemicals, Allentown, PA), observed under a Leitz Ortholux epifluorescence microscope (E. Leitz, Inc., Rockleigh, NJ) equipped with phase optics and photographed with Tri-X 400 ASA film (Eastman Kodak Co., Rochester, NY). The exposures ranged from 15–50 s. Cellular perimeters were measured with a digital planimeter Microplan II (Laboratory Computer Systems Inc., Cambridge, MA). For RIA, cells were plated on 50-well plastic Petri dishes (Lux; Miles Laboratories Inc., Naperville, IL) and processed as described above except that the second antibody was affinity-purified [$^{125}$I]goat anti-mouse IgG, prepared as described elsewhere (52).

### Semithin Frozen Sections

Procedures for semithin frozen sections have been described elsewhere (65, 66). Briefly, MDCK cells were plated on native collagen gels, fixed in 2% PFA, embedded in 10% gelatin in PBS, infused overnight in 1.8 M sucrose/0.4% PFA, frozen in liquid $N_2$, and sectioned in ~0.5-μm-thick sections at −85°C with a Sorvall ultramicrotome with a FS1000 cryoattachment (model MT 5000; Sorvall Instruments Div., Newton, CT). The samples were collected on poly-L-lysine-coated glass coverslips and processed for indirect immunofluorescence as described above.

### Immunoelectronmicroscopy

The immunoperoxidase procedure has been described in detail by Brown and Farquhar (6). In brief, cells were processed as described for immunofluorescence with detergent permeabilization in 0.2% Triton X-100, except that a peroxidase-coupled Fab fragment of rabbit anti-mouse IgG (Biosys, Compiegne, France) was used as second antibody. After fixation in 1% glutaraldehyde, the peroxidase reaction was developed in 50 mg/ml diaminobenzidine (Polysciences Inc., Warrington, PA), 0.06% $H_2O_2$, the cells were postfixed in 1% $OsO_4$, 1% potassium ferrocyanide, and processed for EM. The sections were observed and photographed with a transmission electron microscope (model 100 CX; JEOL USA, Peabody, MA).

## Results

### Time Course of Exocytosis of VAC Upon Establishment of Cell–Cell Contacts

In MDCK monolayers with incomplete intercellular contacts by incubation in 5 μM $Ca^{++}$ (LC), a highly polarized 184-kD apical integral glycoprotein was detected in reduced amounts on the cell surface (38% of control monolayers) by indirect RIA with an mAb. The protein, however, was still polarized to the free surface of these cells. A large intracellular pool of 184-kD protein, 62% of which (as measured by RIA in detergent-permeabilized cells) was found in large vacuoles (VACs) (66). The time course of VAC exocytosis was followed in cells kept for 24 or 48 h in LC and then switched to NC by RIA with 6-h time points over a second 24-h period (see reference 66; Fig. 2). The exocytosed protein included both antigen stored in VAC and a small but significant amount of newly synthesized 184-kD protein. VAC exocytosis was shown to proceed in the presence of cycloheximide, with the shortest time point taken 3 h after calcium switch. This point was not statistically different from the peak at 6 h but it was statistically different from the point at time 0 (see reference 66; Fig. 3 *B*).

In the present work we have studied in detail the kinetic and the early events of VAC exocytosis. We explored the pos-

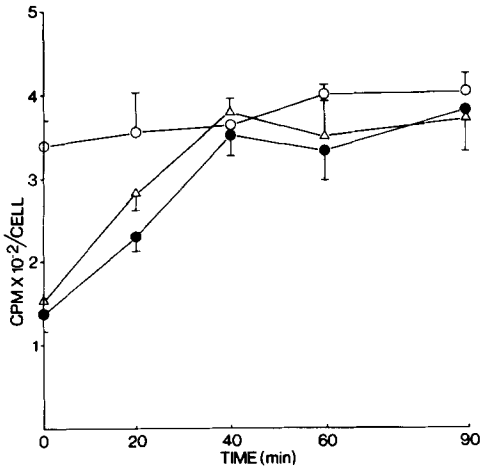


*Figure 1.* RIA determination of the time course of VAC fusion to the plasma membrane after switching from LC to NC. MDCK monolayers kept in LC for 24 h were transferred to NC for various times, fixed in 2% PFA, and processed for indirect RIA with the 184-kD mAb in the first step and affinity-purified [$^{125}$I]goat anti-mouse IgG in the second step. A set of monolayers was permeabilized in 0.2% Triton X-100 in PBS (○) to measure total cellular content of the 184-kD antigen; another set was incubated for 5 min in 2 mM EDTA–PBS (△) before fixation (no detergent); and the 184-kD antigen on the apical surface was measured with no EDTA and no detergent permeabilization (●). The increased surface accessibility of the 184-kD mAb at 20 min after EDTA treatment is significant ($P < 0.02$). Each point shown is the mean value ± SEM of eight samples from three independent experiments.

sibility that VAC exocytosis might proceed faster than previously suspected. To this aim, indirect RIA experiments taking 20-min time points over a 90-min period were performed with an mAb against the apical 184-kD antigen. Since the steady-state cellular content of this antigen is reached in ~24 h, these experiments were performed in the absence of cycloheximide. Fig. 1 shows the time course of 184-kD protein appearance on the cell surface after transfer to NC of MDCK monolayers formed in LC. The intracellular pool of 184-kD protein at $t = 0$ was ~60% of the total cellular content in cells kept in LC medium. This intracellular antigen became accessible to external antibodies within 20–40 min upon transfer to NC (Fig. 1). Exocytosis reached a plateau within 60 min (i.e., considerably faster than suspected from the time course previously published). 30% of the 184-kD protein being exocytosed remained cryptic during the initial 20–30 min, and could only be demonstrated by treatment of the monolayers with 2 mM EDTA for 5 min before fixation and processing for RIA (Fig. 1, △). Since cell–cell contacts and tight junctions develop very rapidly after addition of NC (Table I; see also references 20 and 65), this hidden pool may represent antigen exocytosed toward the developing lateral surface.

### *VAC Exocytosis Occurs at Cell–Cell Contact Sites*

F-actin is a major component of the submembrane cytoskeleton. In epithelial cells it is particularly concentrated in microvilli (14, 42). As expected from their large microvillar content (66), VACs displayed high levels of F-actin detectable with fluorescent phalloidin (Fig. 2, *A* and *D*). While 92% of the cells from monolayers kept in LC for 20 h contain VACs (66), semithin frozen sections detected VACs in approximately one out of every ten cells, due to the relationship between VAC and cell sizes. F-actin was localized to VACs in semithin frozen sections with rhodamine–phalloidin (Fig. 2 *G*); usually weaker fluorescence was observed under both the free and attached plasmalemma (Fig. 2, *G* and *H*). This nonpolarized surface distribution of actin contrasts with the highly polarized apical localization of surface 184-kD antigen under the same circumstances (65; not shown here).

Surprisingly, a small percent of the cell–cell contacts of monolayers kept in LC showed brighter phalloidin fluorescence than the rest of the plasma membrane (Fig. 2 *H*, *arrows*), compatible with the presence of a high microvillar concentration at that level. This suggested spontaneous fusion of VACs toward intercellular spaces. To test directly the hypothesis that VACs fuse toward intercellular spaces, immunofluorescence experiments patterned after the time course of RIAs described before (Fig. 1) were carried out. MDCK monolayers formed in LC were switched to NC for various times, fixed, and processed for 184-kD surface immunofluorescence (EDTA before fixation, no detergent permeabilization). After 40 min in NC, a large number of cells showed VACs accessible to the external antibodies. These VACs had, therefore, fused with the plasma membrane while still preserving their general shape. A characteristic fusion image was observed in most cases, with a rounded bottom end facing the nucleus (Fig. 3, *A–F*, *arrowheads*) and a flat or diffuse border at the level of the cell's edge (Fig. 3, *A–F*, *arrows*). The frequency of cells showing accessible VACs, with characteristic fusion images, was low in LC medium (1 cell out of 194 or 1:194), but increased sharply after 20 min

*Table I. ZO-1 Positive Bands in MDCK Cells Kept in LC*

| Condition | % Totally negative cells | Total cell perimeter | ZO-1 positive cell perimeter | % ZO-1 positive cells | Total number of cells |
|---|---|---|---|---|---|
| | | *μm* | *μm* | | *n* |
| 5 μM $Ca^{++}$ 24 h | 36.4 | 81 ± 22 | 13 ± 15 | 15 ± 18 | 76 |
| 5 μM $Ca^{++}$ 24 h/ 1.8 mM $Ca^{++}$ 40 min | 8.3 | 77 ± 20 | 40 ± 20 | 54 ± 26 | 36 |
| 1.8 mM $Ca^{++}$ 24 h | 0 | 79 ± 23 | 74 ± 19 | 94 ± 12 | 16 |

MDCK cells were cultured and processed for immunofluorescence as described in Fig. 4. The cellular perimeter was measured with a digital planimeter. The perimeter of totally negative cells was included in the statistics. The percent of ZO-1 positive perimeter was calculated on a cell-by-cell basis and then averaged. The data are presented as mean ± SD for *n* cells. The differences of means among ZO-1 positive peripheries in all three conditions were statistically significant ($P < 0.01$, *t* test).

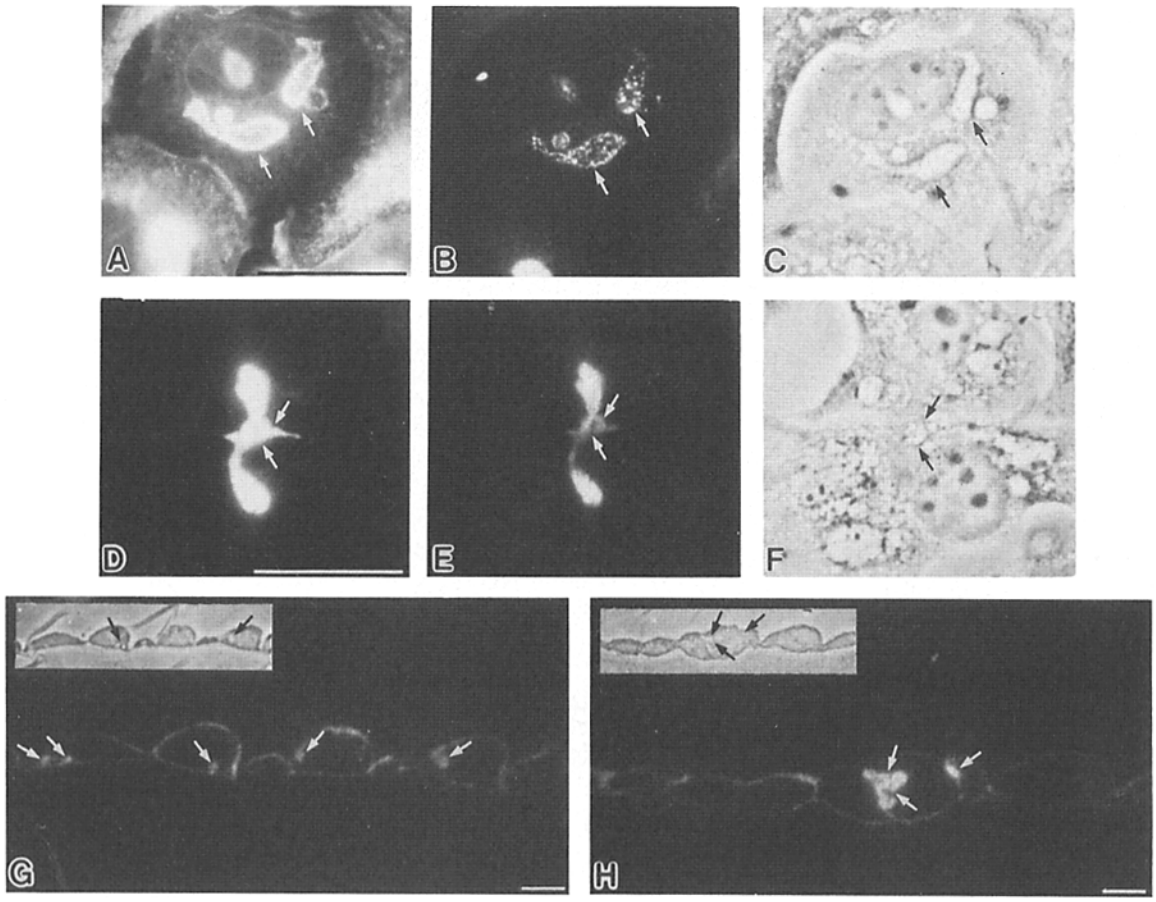


*Figure 2.* Codistribution of F-actin and 184-kD antigen in VAC. MDCK cells were plated in LC on glass coverslips (*A–F*) for en face immunofluorescence or on native collagen gels for frozen sections (*G* and *H*), fixed in 2% PFA–PBS after 24 h, permeabilized in 0.2% Triton X-100 (except the cells for frozen sections), and processed for immunofluorescence with 184-kD mAb (*B* and *E*) and with rhodamine-coupled phalloidin (*A* and *D*). Semithin frozen sections were stained with rhodamine–phalloidin (*G* and *H*). Note codistribution of the 184-kD antigen and F-actin in VACs (*A–F, arrows*), and F-actin concentration in plasma membrane, VACs, and some cell–cell contact areas (*G* and *H, arrows*). Bars: (*A–F*) 8 μm; (*G* and *H*) 15 μm.

(~1:10) and 40 min (1:6) of switch to NC (Fig. 3). At the light microscope level, the fraction of cells showing fusion images after shift to NC never exceeded 20%. Previous work showed that 92% of the cells kept in LC contain VACs (as determined by immunoelectron microscopy and morphometry) and 50% of the cells have VACs detectable by en face fluorescence. On the other hand, no VACs are detectable 2 h after switch from LC to NC (66). Taken together, all these results indicate that the insertion of VACs in the plasma membrane is somewhat asynchronous. The fusion images progressively disappeared after 60 min in NC, with concomitant increase in the apical dotted fluorescence pattern (Fig. 3 *G*) characteristic of confluent monolayers continuously kept in NC.

Although fusion images were observed at the same time as the externalization of the intracellular pool of 184-kD protein, an alternative explanation of these images was recruitment of the antigen fraction already present on the plasma membrane upon shift to NC. To control this possibility we performed the following double fluorescence experiment. MDCK cells were kept in LC medium and preincubated with Fab fragments from 184-kD mAb for 30–40 min. The cells were then switched to NC medium for 30–40 min and fixed. The Fab mAb anti–184-kD was localized with Fab-specific FITC goat anti–mouse antibody (Fig. 3 *I*). The new 184-kD antigen exposed during the period in NC was localized with whole mAb followed by rhodamine–goat anti–mouse IgG (anti-Fc fragment) (Fig. 3 *H*). VAC fusion images labeled with Fab were observed in 1 out of 237 (1:237) cells, which is compatible with the small percent of spontaneous VAC fusion in LC; the frequency observed with the second fluorescent system was ~1:6 cells, in agreement with the results reported above. This experiment indicates that the high frequency "fusion images" observed upon calcium switch actually results from VAC fusion and not from recruitment of the 184-kD antigen from the surface pool.

In summary, the F-actin distribution and the changes in 184-kD protein upon switch from LC to NC suggested that VAC fused at cell–cell contact sites, with displacement of 184-kD antigen and microvilli first toward the developing lateral surface and later toward the definitive apical surface.

### *VAC Fuses on Sites Adjacent to ZO-1–Positive Tight-Junctional Bands*

To further characterize the VAC fusion site, we studied its

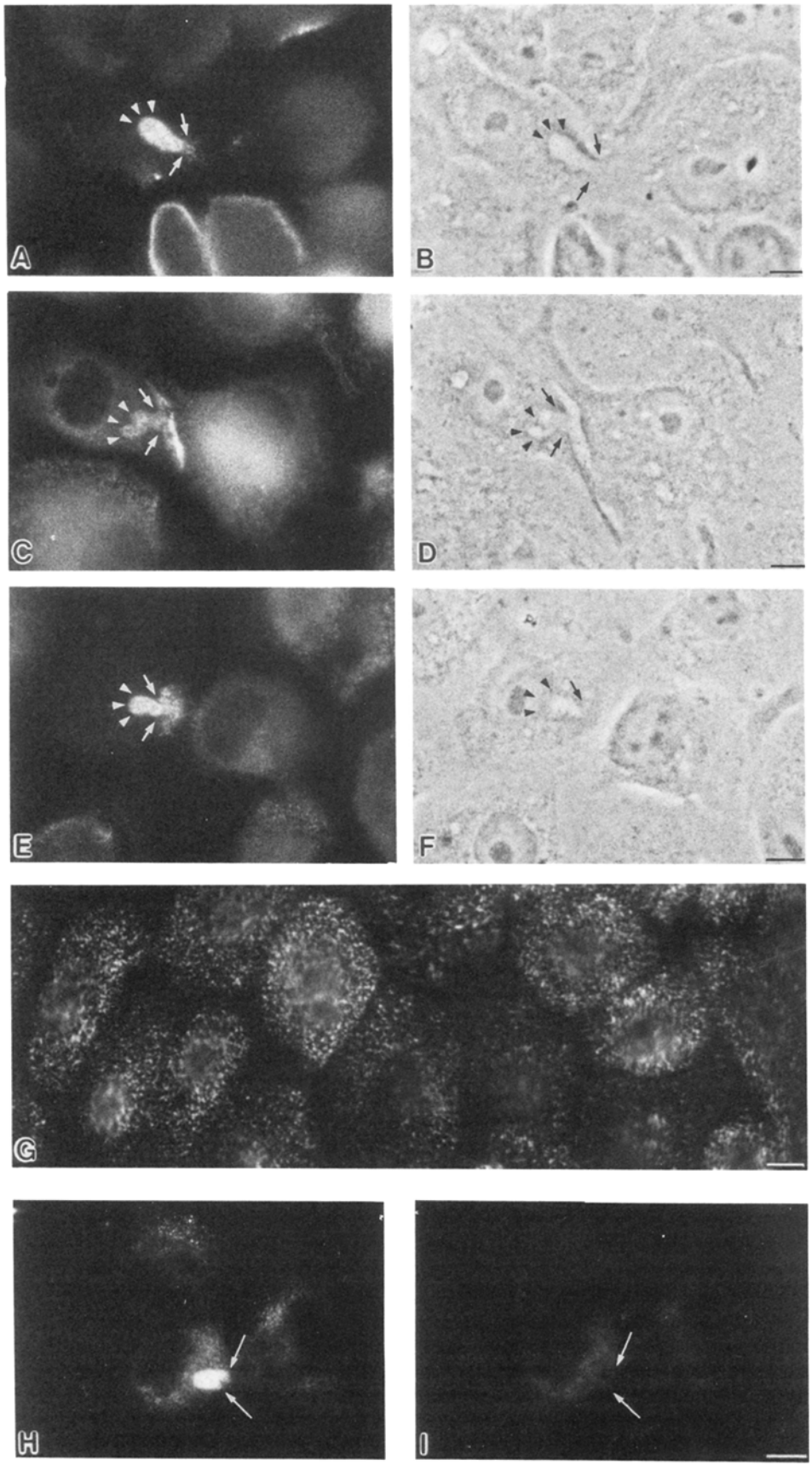


*Figure 3.* Immunofluorescence localization of 184-kD antigen during VAC fusion with the plasma membrane. MDCK cells were kept in LC for 24 h, switched to NC for 40 min, treated with 2 mM EDTA in PBS for 5 min, and fixed in 2% PFA in PBS (*A–F*). Parallel monolayers were fixed after 24-h incubation in NC (*G*). The cells were processed for indirect immunofluorescence with 184-kD mAb without detergent permeabilization. Some cells were preincubated with anti-184-kD mAb Fab fragments before calcium switch (*H* and *I*). After 30–40 min in NC these cells were fixed and sequentially processed with fluorescein-coupled anti-mouse Fab IgG, normal mouse IgG Fab fragments, whole anti-184-kD mAb, and rhodamine-coupled anti-mouse Fc fragment. The same cells were photographed using the rhodamine filter (*H*, 184-kD protein exocytosed after calcium switch) or the fluorescein filter (*I*, 184-kD protein present on the surface before calcium switch). *Arrowheads*, the bottom end of VACs fused with the plasma membrane as demonstrated by their accessibility to external antibodies. *Arrows*, presumptive fusion sites as determined by the irregular border and spreading of the 184-kD membrane protein on the plasma membrane. Fusion always occurred at cell–cell contact areas. Bars, 4 μm.

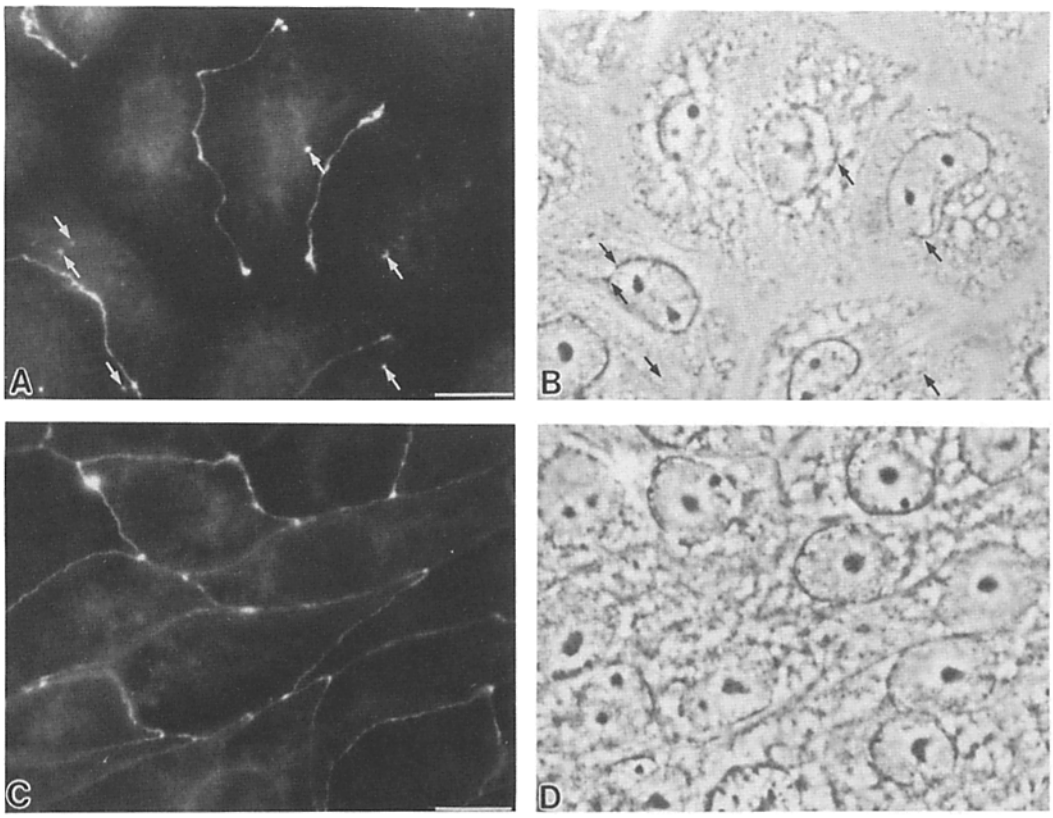


*Figure 4.* Immunofluorescence localization of tight-junctional antigen ZO-1 in confluent MDCK cell monolayers kept in LC or NC. MDCK cells were incubated in LC (*A* and *B*) or NC (*C* and *D*) for 24 h, fixed in 96% methanol at −20°C, and processed for immunofluorescence with ZO-1 rat mAb and affinity-purified goat anti-rat IgG coupled to rhodamine. ZO-1 positive bands appeared between cells, but the arrows point at ZO-1 positive "dots" (*A*) in close association with VACs identified in the corresponding phase image (*B*). Bar, 5 μm.

spatial relationship to the developing tight junctions, localized with a rat mAb against ZO-1, a 225-kD antigen recently described by Stevenson et al. (57). This antibody recognizes both the native and the SDS-denatured forms of ZO-1, but not the aldehyde-fixed form; since ZO-1 is a peripheral cytoplasmic protein, the cells were fixed with methanol, instead of PFA, to allow access of the antibodies. As described by Stevenson et al., ZO-1 was localized to a continuous thin band around the apical borders of confluent MDCK cells (Fig. 4, *C* and *D*). In subconfluent MDCK monolayers, ZO-1 fluorescent bands were strictly localized to areas of cell–cell contact in cell pairs or triplets; these bands were never observed in single cells (data not shown). In MDCK monolayers formed for 20 h in LC medium, ZO-1 was observed as discontinuous, relatively infrequent short lines along cell borders (Fig. 4, *A* and *B*), and in small fluorescent dots closely associated with VAC phase images (Fig. 4, *A* and *B*, *arrows*). We have no explanation for the significance of these ZO-1 structures associated with VACs. 36% of the cells showed no ZO-1 positive bands at all, and only 15% of the average cellular perimeter was positive for ZO-1 (Table I). This correlates well with our previous data reporting on a small percent (13%) of ruthenium red–excluding cell contacts present in MDCK cells kept in LC (65). Upon shift to NC, ZO-1 positive bands rapidly organized. Only 8% of the cells were totally negative for ZO-1 after 40 min in NC, and the average positive perimeter was 54% (Table I). This 40-min half-time of organization of tight junctions correlates well with the timing of VAC exocytosis, suggesting that both phenomena depend on a common trigger: the establishment of extensive cell–cell contacts at the level of the developing lateral domain.

To test the possibility that VAC fusion sites were related to these ZO-1 positive bands, double fluorescence experiments with anti–ZO-1 rat mAb and 184-kD mouse mAb were carried out. In MDCK monolayers kept in NC, the two antigens showed a complementary distribution: the 184-kD antigen was localized on the apical domain, but partially excluded from cell borders and the peripheral ~1 μm of the apical surface, while ZO-1 was seen precisely at the cell borders (Fig. 5, *A* and *B*, *arrows*). Upon shift from LC to NC, VAC fusion sites were always localized adjacent to ZO-1 positive cell contact areas (Fig. 5, *C* and *D*, *arrows*). However, ZO-1 was excluded from the fusion sites themselves (Fig. 5, *F* and *G*, *arrows*). This relationship was particularly striking in cells with small ZO-1 positive bands. In these cells, VACs were usually observed between the nucleus and the ZO-1 positive band, fusing to a site in the cell border always immediately adjacent to the ZO-1 strand (Fig. 5, *I*, *J*, and *K*). Since at 40 min after shift to NC 46% of the cell perimeter was still negative for ZO-1, one would expect the same proportion of VACs fusing toward ZO-1 negative areas. The absence of VACs associated with ZO-1 negative cellular perimeters indicates a strong correlation between fusion sites and ZO-1 bands, a marker for cell–cell contact areas.

In the above mentioned experiments, the cells were per-

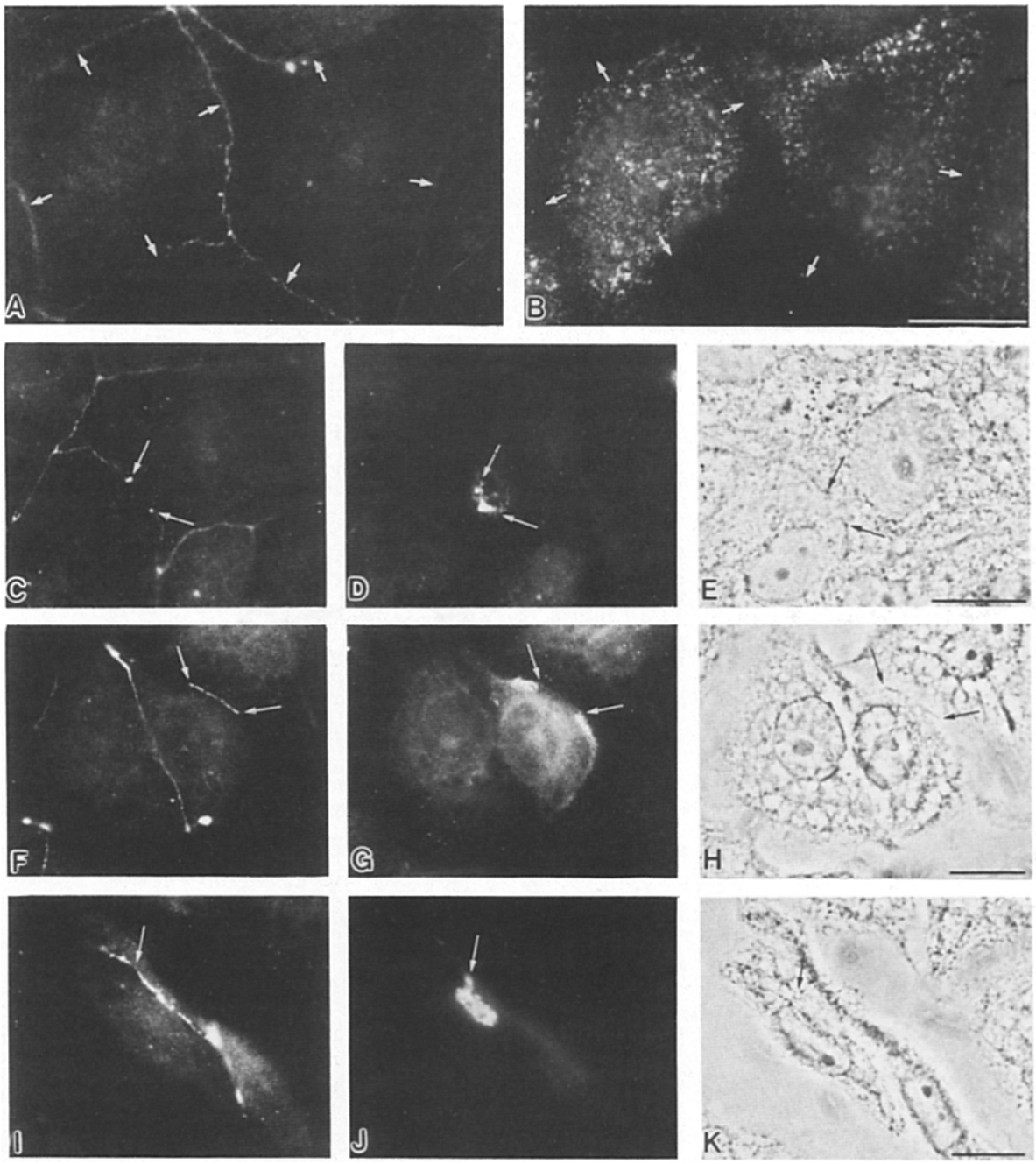


*Figure 5.* VAC is inserted close to ZO-1 positive bands at cell–cell contact areas. MDCK cells were incubated in NC for 24 h (*A* and *B*) or kept in LC for 24 h and switched for 40 min to NC (*C–K*), fixed in 96% methanol at −20°C, and processed for double immunofluorescence. They were sequentially exposed to ZO-1 rat mAb, rhodamine-conjugated goat anti-rat Ig, 184-kD mouse mAb, and fluorescein-conjugated goat anti-mouse Ig. No second antibody cross-reactivity was observed. ZO-1 (rhodamine) fluorescence (*A*, *C*, *F*, and *I*) and 184-kD mAb (fluorescein) fluorescence (*B*, *D*, *G*, and *J*) from the same fields. In *A* and *B*, the arrows point at cell–cell contacts. In *C–K*, the arrows delimit the VAC fusion sites on the plasma membrane directly next to ZO-1 positive areas. Note that in cells with a portion of the perimeter negative for ZO-1, VAC localized towards the ZO-1 positive band at cell–cell contacts (*I* and *J*). Bars, 7 μm.

meabilized before addition of 184-kD antibody for immunofluorescence; therefore some of the VAC images might correspond to unfused vacuoles. However, the RIA results (Fig. 1) indicate that 40 min after calcium switch >95% of the intracellular 184-kD antigen has been inserted on the cell surface. Thus, >95% of the VACs showed in these experiments correspond to the fusion images in Fig. 3. Since ZO-1 can be considered a reliable marker for cell–cell contacts, these data indicate that VAC fusion occurs, indeed, toward intercellular spaces and that VACs distribute in a polarized fashion between nuclei and the intercellular contacts. No conclusions can be drawn, however, on a possible direct involvement of tight junctional components in VAC fusion.

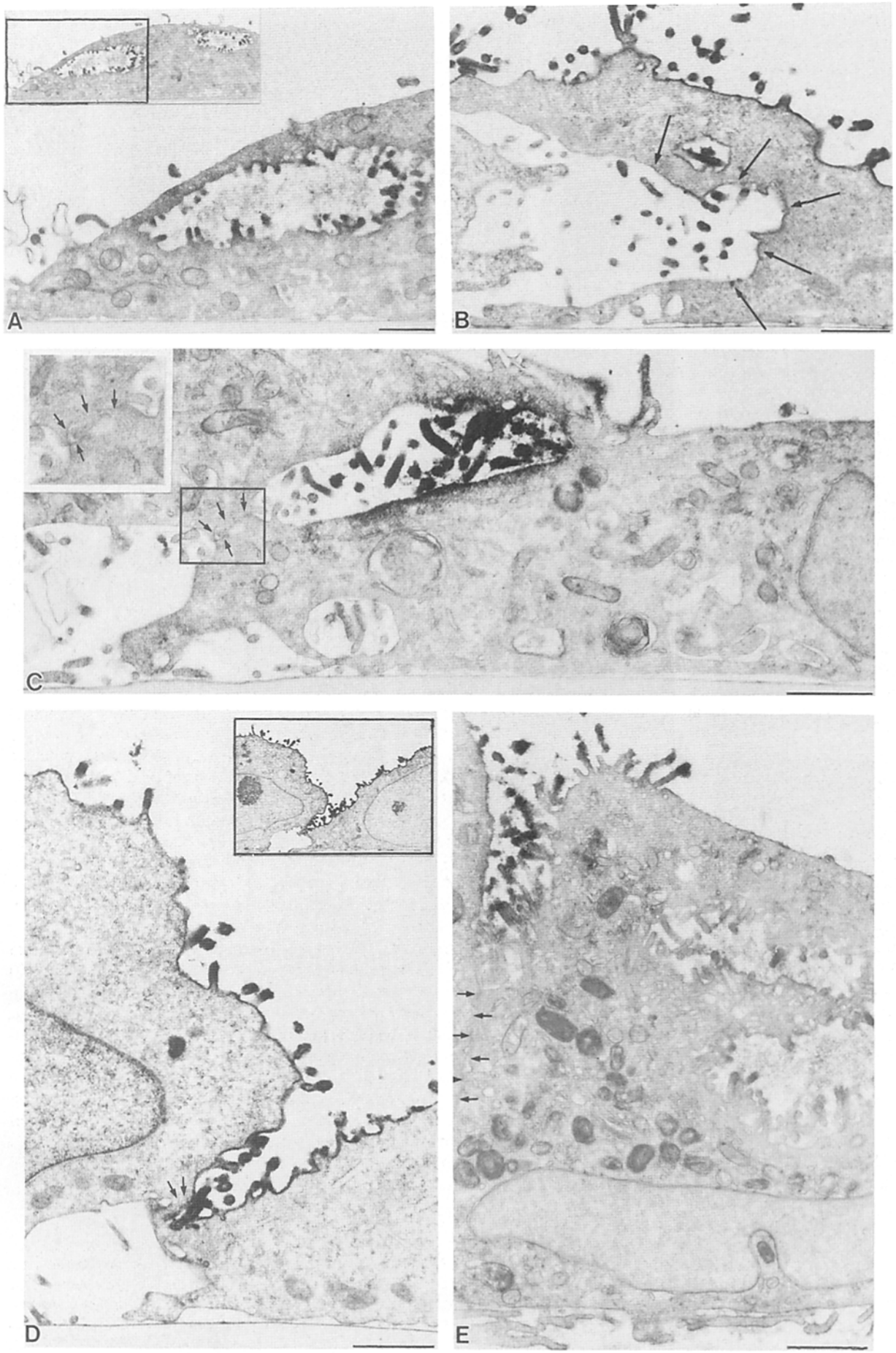
A
B
C
D
E

### *Establishment of the Apical Domain from VAC Fusion Sites at the Cell–Cell Contact Surface*

Immunoperoxidase experiments at the EM level confirmed the fluorescence observations. In cells kept in LC (before switch to NC), VACs were found throughout the cytoplasm. Many VACs were juxtanuclear while others were found close to the cell periphery (Fig. 6 *A*, and corresponding inset; see also Figs. 4, *A*, *C*, and *E*; and 5, *A* and *E* in reference 66). Since the free (apical) surface accounts for 57% of the total plasma membrane surface and the lateral for just 16% in cells kept in LC (65), the chances of a random fusion of VAC with the plasma membrane would largely favor a direct fusion anywhere in the free surface. Strikingly, this was not the case. As strongly suggested by the fluorescence experiments, no VAC was observed fusing away from cell–cell contact areas. Rather, upon switch from LC to NC, numerous images of microvilli with positive immunoperoxidase reaction for the 184-kD membrane protein were observed in lateral spaces between cells (Fig. 6, *B* and *C*), frequently limited by cell–cell contacts (Fig. 6 *C*, *arrows*). These lateral pockets with microvilli were clearly transient since they were never observed in cells continuously kept in NC or after 6 h of switch from LC to NC. 40 min after shift to NC, bunches of microvilli with 184-kD protein were often observed between lateral and apical surfaces (Fig. 6, *D* and *E*). Although continuities between intracellular and surface areas with microvilli in the three-dimensional structure are likely (i.e., Fig. 6 *E*), such bunches of microvilli between both domains are never observed in monolayers continuously kept in NC. Since it has been shown at the fluorescence level that the calcium switch does not cause recruitment of the 184-kD apical protein, these transitional images must necessarily correspond to the displacement of apical material from the lateral surface to its final destination in the apical surface.

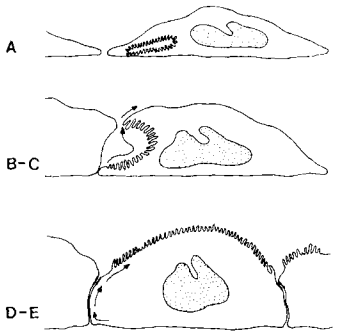


*Figure 7.* Steps in the exocytosis of VAC and of the establishment of apical plasma membrane from precursor VACs. *A–E* correlate with immunoperoxidase panels in Fig. 6. See text for explanation.

## *Discussion*

### *VAC Exocytosis and the Establishment of the Apical Domain*

The RIA, immunofluorescence, and immunoelectron microscopy results in this report suggest the model of VAC exocytosis and formation of the apical domain depicted in Fig. 7. In the absence of complete cell–cell contacts, MDCK cells develop large vacuoles (VACs) rich in structural and biochemical apical markers, such as 184-kD protein, microvilli, F-actin, and, presumably, other components of the apical surface cytoskeleton (Fig. 7 *A*, see actual data in Fig. 6 *A*). Under these conditions the free surface contains only a restricted set of its components (i.e., averaging 38% of the total cellular 184-kD protein, although there is cell heterogeneity: some cells keep the antigen mostly in VACs showing a negative surface; compare Fig. 4, *A* and *C*, and Fig. 5, *A* and *B*, in reference 65). Presumably, these components reach the surface by a mechanism that bypasses VAC, perhaps the same process that operates in NC. Establishment of extensive cell–cell contacts triggers VAC externalization toward the developing (primitive) lateral surface; fusion takes place in areas adjacent to tight junctional bands identified by the specific antigen ZO-1 (Fig. 7 *B*; see actual data in Figs. 2 *H* and 5; and Fig. 6, *B* and *C*). Transient microvilli-rich intercellular pockets, resembling intercellular (secondary) lumina described in developing epithelia (13, 37, 39) are observed at this stage. A small fraction of these pockets may be transiently sealed off, becoming accessible to apical antibodies only in the presence of EDTA (Fig. 1). Whether tight junctions are the sealing element is not clear from the current data. Most of the pockets, however are readily accessible to the antibodies (Fig. 3, *A*, *C*, and *E*).

Since 84% of the cell surface in LC corresponds to free (apical) plus basal domains (65), the probability of a VAC fusing precisely toward the cell–cell contact area (16%) just by chance is very low. Even lower is the probability of fusing with regions adjacent to ZO-1 bands, since these exist in ~14% of the cell perimeter in LC (Table I). Fragmented tight junctional strands were also observed by freeze-fracture EM by Gonzalez-Mariscal et al. (20). Recent fluorescence recovery after photobleaching experiments indicate, however, that some kind of filtering mechanism prevents the diffusion of at least one freely mobile apical membrane protein from the free to the attached surface (52a). The nature of this structure and its relationship with the definitive tight junction are still unknown.

Tight junctions develop quickly after transfer from LC to NC. Transmonolayer resistance develops within 2–4 h (20) but much earlier, after 40 min, ZO-1 positive bands are observed around >50% of the cell border. We have, as yet, no evidence on the nature of the force that approaches VACs toward cell–cell contact areas, or on whether tight junctions may be directly involved. As all the fusion events we have observed in both immunofluorescence and immunoelectron microscopy experiments occurred toward developing lateral spaces, we conclude that the topological organizer of VAC exocytosis must be present only where two neighboring cells touch each other.

*Figure 6.* VAC fusion to the plasma membrane and shift of apical markers to the free cell surface: immunoperoxidase localization of 184-kD antigen. MDCK cells were incubated for 24 h in LC (*A*). Some monolayers were switched to NC for 30 min (*B–E*). All the samples were fixed, permeabilized with Triton X-100, and processed for indirect immunoperoxidase EM with 184-kD mAb and Fab goat anti-mouse IgG coupled to peroxidase. (*B*) *Long arrows*, 184-kD protein positive membrane, presumably a VAC fusion site. (*C–E*) *Short arrows*, cell–cell contacts as determined by the presence of two plasma membrane sections (*inset* in *C* and *E*) or two nuclei (*inset* in *D*). Bars, 1 μm.

Finally, the block of newly incorporated apical plasma membrane moves to its final localization in the free surface (Fig. 7 *D*; see actual data in Fig. 6, *C*, *D*, and *E*). The mechanism, somewhat asynchronous, reaches this stage in ~40 min after calcium replacement. The shift of membrane components of the intercellular pocket toward the free apical surface is completed within 2 h. Although the EM images shown in Fig. 6 suggest a bulk membrane movement, our data do not allow us to rule out a slow lateral diffusion process at the molecular level. We speculate that the lateral domain develops simultaneously with this last event, by redistribution of basolateral components and/or insertion of specific lateral components (i.e., desmosomes; see reference 56) and the sealing of tight junctions behind the moving apical block. Since actin and presumably other membrane-associated apical cytoskeletal components colocalize with VACs, the role of the cytoskeleton as driving (and perhaps regulating) structure for VAC–surface fusion remains an interesting possibility.

### *Regulation of VAC Fusion With the Plasma Membrane*

It is unclear how the establishment of cell contacts leads to the large redistribution of surface and intracellular membranes associated with the exocytosis of VAC. It may be speculated that receptors for neighboring cells, such as cell adhesion molecules (16, 44), play a crucial role in this process, perhaps through the release of an intracellular messenger. The calcium-dependent cell adhesion molecule uvomorulin, present in kidney epithelium (67), is a major organizer of the lateral domain of MDCK cells (23). Blocking uvomorulin with specific antibodies prevents the formation of cell contacts in MDCK cells (3, 29) and even the development of tight junctions (22). Therefore, switching from LC to NC would result in the rapid (<2 h, see reference 65) formation of lateral domains and tight junctions by allowing the operation of uvomorulin (22) and/or other cell adhesion molecules. These events have been shown to correlate with the deposition of an insoluble fodrin network at the lateral membrane (43). It is still unclear whether the trigger for VAC fusion is calcium dependent itself or secondarily dependent on the organizing role of calcium-dependent cell adhesion molecules; i.e., it is conceivable that a weak calcium-independent mechanism may be involved in cell–cell recognition and that such a mechanism may require the synergic operation of calcium-dependent adhesive forces. These possibilities are currently under investigation.

### *Biological Significance of VAC*

Unlike the situation in fully polarized epithelial monolayers, where polarity is maintained by intracellular sorting and specific targeting mechanisms (8, 40, 41, 45, 50, 53) mediated by small vesicles (100–200 nm) carrying plasma membrane components (21, 52), VAC (3.6 ± 1.3 μm in diameter) participates in the establishment of the apical domain in cells lacking definitive plasma membrane domains. Our data do not rule out the possible operation of the mechanism mediated by small vesicles in cells kept in LC medium, although these vesicles have seldom been observed in our immunoelectron microscopy experiments with cellular markers.

Mathan et al. (39), as well as Neutra and co-workers (13, 37) have shown that fetal intestinal glands develop as solid cell cords with no lumina; "secondary" lumina containing alkaline phosphatase appear in cell–cell contact areas and later coalesce into one single lumen. Similar events have been described during the development of kidney tubules (18), seminiferous tubules (5, 54), thyroid follicles (10), submandibular gland (11), and mammary gland (15). We propose that the mechanism of VAC exocytosis described in this report is the same as that responsible for epithelial lumen formation during development. This mechanism, as well as other differentiation processes (4, 26, 35, 36, 64) seems to be very strictly controlled by cell–cell contacts.

The presence of VACs in MDCK cells (and perhaps also in LLCPK cells; Salas, P. J. I., D. E. Vega-Salas, A. Patzak, M. Roth, and E. Rodriguez-Boulan, unpublished observations), may be related to the loss of differentiated properties associated with becoming a cell line. MDCK cells show evidence of dedifferentiation because some of their surface antigens are not present in adult dog kidney tubules (Vega-Salas, D. E., P. J. I. Salas, and E. Rodriguez-Boulan, unpublished results) and because they can form tumors after injection in nude mice (34), although this result is still controversial (58, 59). Intracellular lumina have also been observed in a variety of tumor cells of epithelial lineage (7, 47, 60, 61, 63). In this case, dedifferentiating cells may be defective in the cell–cell contact mechanism that triggers VAC exocytosis. In fact, epithelial tumor cells are less adhesive and thus capable of leaving their original tissue and forming metastasis (2, 28). Further work is needed to establish whether the VAC mechanism is present only in dedifferentiating cells or if it is a function common to epithelial cells during normal differentiation; as well as to elucidate the molecular basis of this interesting mechanism involved in key aspects of the generation of surface polarity by epithelial cells.

The authors dedicate this work to the memory of the admired scientist, teacher, and Nobel awardee, Dr. Luis F. Leloir, who passed away on 12/2.

We are especially grateful to Dr. Daniel Goodenough (Harvard Medical School, Boston, MA) for providing anti-ZO-1 antibody and helpful criticisms. We thank Drs. Marian Neutra (Harvard Medical School), Donald A. Fischman, Doris Wall, and Joel Pardee for encouraging discussion and providing fluorescent probes. We also thank Mr. James Denis for excellent electron microscopy and Mr. Wayne Fries for skillful technical assistance.

This work was supported by grants from the National Institutes of Health (GM-34107), National Science Foundation (PCM-8217405), New York Heart Association, Consejo Nacional de Investigaciones Científicas y Tecnicas (CONICET) (PIA 019/87), Fundación A. J. Roemmers (Argentina), and the generous contribution from Drs. Maria E. Francou de Siniscalchi and Miguel R. Siniscalchi. P. J. I. Salas and D. E. Vega-Salas are Career Investigators at CONICET (Argentina). E. Rodriguez-Boulan is recipient of an Established Investigator award from the American Heart Association.

Received for publication 25 September 1987, and in revised form 18 July 1988.

#### *References*

1. Alluchon-Gerard, M. J. 1979. Morphogenese ultrastructurale et differenciation fonctionnelle du follicule thyroidien de la Roussette. *Arch. Anat. Microsc. Morphol. Exp.* 68:43–60.
2. Alroy, J., B. U. Pauli, and R. S. Weinstein. 1981. Correlation between numbers of desmosomes and the aggressiveness of transitional cell carcinoma in human urinary bladder. *Cancer (Phila.).* 47:104–112.
3. Behrens, J., W. Birchmeier, S. L. Goodman, and B. A. Imhoff. 1985. Dissociation of Madin-Darby canine kidney epithelial cells by the monoclonal antibody anti-Arc-1: mechanistic aspects and identification of the antigen as a component related to uvomorulin. *J. Cell Biol.* 101:1307–1315.

4. Ben-Ze'ev, A. 1984. Differential control of cytokeratins and vimentin synthesis by cell-cell contact and cell spreading in cultured epithelial cells. *J. Cell Biol.* 99:1424–1433.
5. Bressler, R. S., and I. J. Lustbader. 1978. Effect of testosterone on development of the lumen in seminiferous tubules of the rat. *Andrologia.* 10: 291–298.
6. Brown, W. J., and M. G. Farquhar. 1984. The mannose-6-phosphate receptor for lysosomal enzymes is concentrated in cis-golgi cisternae. *Cell.* 36:295–307.
7. Capella, C., B. Frigerio, M. Cornaggia, E. Solcia, Y. Pinzon-Trujillo, and G. Chejfec. 1984. Gastric parietal cell carcinoma: a newly recognized entity: light microscopic and ultrastructural features. *Histopathology (Oxf.).* 8:813–824.
8. Caplan, M. J., H. C. Anderson, G. E. Palade, and J. D. Jamieson. 1986. Intracellular sorting and polarized cell surface delivery of ($Na^+$-$K^+$)ATPase, an endogenous component of MDCK cell basolateral plasma membranes. *Cell.* 24:24–32.
9. Cereijido, M., E. S. Robbins, W. J. Dolan, C. A. Rotunno, and D. D. Sabatini. 1978. Polarized monolayers formed by epithelial cells on a permeable and translucent support. *J. Cell Biol.* 77:853–880.
10. Chan, A. S. 1983. Ultrastructural observations on the formation of follicles in the human fetal thyroid. *Cell Tissue Res.* 233:693–698.
11. Chaudhry, A. P., L. S. Cutler, J. A. Schmutz, Jr., G. M. Yamane, L. K. Pierri, and M. Sunderraj. 1986. Development of the hamster submandibular gland. II. The ductal system. *J. Submicrosc. Cytol.* 18:529–536.
12. Chomette, G., M. Auriol, A. Delcourt, and Y. Terean. 1980. Contribution a l'histogenese du cancer lobulaire du sein. Etude histoenzymologique et ultrastructurale d'un epithelium invasif a cellules mucipares. *Ann. Anat. Pathol.* 25:85–94.
13. Colony, P. C., and M. R. Neutra. 1983. Epithelial differentiation in the fetal rat colon. I. Plasma membrane phosphatase activities. *Dev. Biol.* 97: 349–363.
14. Drenckhahn, D., and H. Franz. 1986. Identification of actin, alpha-actinin, and vinculin-containing plaques at the lateral membrane of epithelial cells. *J. Cell Biol.* 102:1843–1852.
15. Dulbecco, R., W. R. Allen, and M. Bowman. 1984. Lumen formation and redistribution of inframembranous proteins during differentiation of ducts in the rat mammary gland. *Proc. Natl. Acad. Sci. USA.* 81:5763–5766.
16. Edelman, G. M. 1986. Cell adhesion molecules in the regulation of animal form and tissue pattern. *Annu. Rev. Cell Biol.* 2:81–116.
17. Edidin, M., and T. Wei. 1982. Lateral diffusion of H-2 antigens on mouse fibroblasts. *J. Cell Biol.* 95:458–462.
18. Ekblom, P. 1981. Determination and differentiation of the nephron. *Med. Biol. (Helsinki).* 59:139–160.
19. Ekholm, R., and U. Bjorkman. 1984. Localization of iodine binding in the thyroid gland in vitro. *Endocrinology.* 115:1558–1567.
20. Gonzalez-Mariscal, L., B. Chavez de Ramirez, and M. Cereijido. 1985. Tight-junction formation in cultured epithelial cells (MDCK). *J. Membr. Biol.* 86:113–125.
21. Griffiths, G., S. Pfeifer, K. Simons, and K. Matlin. 1985. Exit of newly synthesized membrane proteins from the *trans* cisterna of the golgi complex to the plasma membrane. *J. Cell Biol.* 101:949–964.
22. Gumbiner, B., and K. Simons. 1986. A functional assay for proteins involved in establishing an epithelial occluding barrier: identification of an uvomorulin-like polypeptide. *J. Cell Biol.* 102:457–468.
23. Gumbiner, B., and K. Simons. 1987. The role of uvomorulin in the formation of epithelial occluding junctions. *Ciba Found. Symp.* 125:168–186.
24. Hall, H. G., D. A. Farson, and M. J. Bissell. 1982. Lumen formation by epithelial cell lines in response to collagen overlay: a morphogenetic model in culture. *Proc. Natl. Acad. Sci. USA.* 79:4672–4676.
25. Handler, J. S. 1983. Use of cultured epithelia to study transport and its regulation. *J. Exp. Biol.* 106:55–69.
26. Heimark, R. L., and S. M. Schwartz. 1985. The role of membrane–membrane interactions in the regulation of endothelial cell growth. *J. Cell Biol.* 100:1934–1940.
27. Herzlinger, D. A., and G. Ojakian. 1984. Studies on the development and maintenance of epithelial cell surface polarity with monoclonal antibodies. *J. Cell Biol.* 98:1777–1787.
28. Hirano, I., and H. Kachi. 1967. The significance of mutual adhesiveness of cells in the histological pattern of cancer tissues. *Acta Pathol. Jpn.* 17:7–21.
29. Imhoff, B. A., H. P. Vollmers, S. L. Goodman, and W. Birchmeir. 1983. Cell-cell interaction and polarity of epithelial cells: specific perturbation using a monoclonal antibody. *Cell.* 35:667–675.
30. Johannessen, J. V., V. E. Gould, and J. Wellington. 1978. The fine structure of human thyroid cancer. *Hum. Pathol.* 9:358–400.
31. Kondo, K., H. Tamura, and H. Taniguchi. 1970. Intracellular microcysts in gastric cancer cells. *J. Electron. Microsc.* 19:41–49.
32. Kondo, Y., T. Akita, I. Sugano, and K. Isono. 1984. Signet ring cell carcinoma of the breast. *Acta Pathol. Jpn.* 34:875–880.
33. Langer, M. 1979. Histological study of the teleost liver. III. The system of biliary pathways. *Z. Mikrosk. Anat. Forsch. (Leipz.).* 93:1105–1136.
34. Leighton, J., L. W. Estes, S. Mansukhani, and Z. Brada. 1970. A cell line derived from normal dog kidney (MDCK) exhibiting qualities of papillary adenocarcinoma and renal tubular epithelium. *Cancer (Phila.).* 26: 1022–1028.
35. Levine, J. F., and F. E. Stockdale. 1985. Cell–cell interactions promote mammary epithelial cell differentiation. *J. Cell Biol.* 100:1415–1422.
36. Louvard, D. O. 1980. Apical membrane amino peptidase appears at site of cell-cell contact in cultured kidney epithelial cells. *Proc. Natl. Acad. Sci. USA.* 77:4132–4136.
37. Madara, J. L., M. R. Neutra, and J. S. Trier. 1981. Junctional complexes in fetal rat small intestine during morphogenesis. *Dev. Biol.* 86:170–178.
38. Madin, S. H., and N. B. Darby. 1988. As catalogued. *In* American Type Culture Collection Catalog of Cell Lines and Hybridoma Strains. 6th Ed. R. Hay, M. Macy, T. R. Chen, P. McClintock, and Y. Reid, editors. ATCC, Rockville, MD. 19–20.
39. Mathan, M., P. C. Moxey, and J. S. Trier. 1976. Morphogenesis of fetal rat duodenal villi. *Am. J. Anat.* 146:73–92.
40. Matlin, K. S., D. Bainton, M. Pesonen, N. Genty, D. Louvard, and K. Simons. 1983. Transfer of a viral envelope glycoprotein from the apical to the basolateral plasma membrane of MDCK cells. I. Morphological evidence. *J. Cell Biol.* 97:627–637.
41. Misek, D. M., E. Bard, and E. Rodriguez-Boulan. 1984. Biogenesis of epithelial cell polarity. Intracellular sorting and vectorial exocytosis of an apical plasma membrane protein. *Cell.* 39:537–546.
42. Mooseker, M. S. 1985. Organization, chemistry, and assembly of the cytoskeletal apparatus of the intestinal brush border. *Annu. Rev. Cell Biol.* 1:209–241.
43. Nelson, W. J., and P. J. Veshnock. 1986. Dynamics of membrane-skeleton (fodrin) organization during development of polarity in Madin-Darby canine kidney cells. *J. Cell Biol.* 103:1751–1766.
44. Odin, P., and B. Obrink. 1986. Dynamic expression of the cell adhesion molecule cell-CAM 105 in fetal and regenerating rat liver. *Exp. Cell Res.* 164:103–114.
45. Pfeiffer, S., S. D. Fuller, and K. Simons. 1985. Intracellular sorting and basolateral appearance of the G protein of vesicular stomatitis virus in Madin-Darby canine kidney cells. *J. Cell Biol.* 101:470–476.
46. Pic, P., L. Remy, A.-M. Athouel-Haon, and E. Mazzella. 1984. Evidence for a role of the cytoskeleton in the in vitro folliculogenesis of the thyroid gland of the fetal rat. *Cell Tissue Res.* 237:499–508.
47. Remy, L. 1986. The intracellular lumen: origin, role, and implications of a cytoplasmic neostructure. *Biol. Cell.* 56:97–106.
48. Remy, L., and J. Marvaldi. 1985. Origin of intracellular lumina in HT 29 colonic adenocarcinoma cell line. An ultrastructural study. *Virchows Arch. B Cell Pathol.* B48:145–153.
49. Remy, L., M. Michel-Bechet, C. Cataldo, J. Bottini, S. Hovsepian, and G. Fayet. 1977. The role of intracellular lumina in thyroid cells for follicle morphogenesis in vitro. *J. Ultrastr. Res.* 61:243–253.
50. Rindler, M. J., I. E. Ivanov, H. Plesken, and D. D. Sabatini. 1985. Polarized delivery of viral glycoproteins to the apical and basolateral plasma membranes of Madin-Darby canine kidney cells infected with temperature-sensitive viruses. *J. Cell Biol.* 100:136–151.
51. Rodriguez-Boulan, E. 1983. Membrane biogenesis: enveloped RNA viruses and epithelial polarity. *Mod. Cell Biol.* 1:119–170.
52. Rodriguez-Boulan, E., K. T. Paskiet, P. J. I. Salas, and E. Bard. 1984. Intracellular transport of influenza virus hemagglutinin to the apical surface of Madin-Darby canine kidney cells. *J. Cell Biol.* 98:308–319.
52a. Salas, P. J. I., D. E. Vega-Salas, J. Hochman, E. Rodriguez-Boulan, and M. Edidin. 1988. Selective anchoring in the specific plasma domain: a role in epithelial cell polarity. *J. Cell Biol.* In press.
53. Salas, P. J. I., D. E. Vega-Salas, D. E. Misek, E. Bard, and E. Rodriguez-Boulan. 1984. Intracellular sorting of plasma membrane glycoproteins in epithelial cells. *Ann. NY Acad. Sci.* 435:337–340.
54. Schulze, W., and U. Rehder. 1984. Organization and morphogenesis of the human seminiferous epithelium. *Cell Tissue Res.* 237:395–407.
55. Simons, K., and S. D. Fuller. 1985. Cell surface polarity in epithelia. *Annu. Rev. Cell Biol.* 1:243–288.
56. Steinberg, M. S., H. Shida, G. J. Giudice, M. Shida, N. H. Patel, and O. W. Blaschuk. 1987. On the molecular organization, diversity and functions of desmosomal proteins. *Ciba Found. Symp.* 125:3–25.
57. Stevenson, B. R., J. D. Siliciano, M. S. Mooseker, and D. A. Goodenough. 1986. Identification of ZO-1: a high molecular weight polypeptide associated with the tight junction (zonula occludens) in a variety of epithelia. *J. Cell Biol.* 103:755–766.
58. Stiles, C. D., W. Desmond, L. M. Chuman, G. Sato, and M. Saier. 1976. Growth control of heterologous tissue culture cells in the congenitally athymic nude mouse. *Cancer Res.* 36:1353–1360.
59. Stiles, C. D., W. Desmond, L. M. Chuman, G. Sato, and M. Saier. 1976. Relationship of cell growth behavior in vitro to tumorigenicity in athymic nude mice. *Cancer Res.* 36:3300–3305.
60. Deleted in proof.
61. Taxy, J. B., H. Battifora, and R. Oyasu. 1974. Adenomatoid tumors: a light microscopic, histochemical and ultrastructural study. *Cancer (Phila.).* 34:306–316.
62. Trump, B. F., B. M. Heatfield, P. D. Phelps, H. Sanefuji, and A. F. Shamsuddin. 1980. Cell surface changes in preneoplastic and neoplastic epithelium. *Scanning Electron Microsc.* 111:43–60.

63. Tsuchiya, S. 1981. Intracytoplasmic lumina of human breast cancer. *Acta Pathol. Jpn.* 31:45–54.
64. Tung, P., and I. Fritz. 1986. Cell-substratum and cell-cell interactions promote testicular peritubular myoid cell histotypic expression in vitro. *Dev. Biol.* 115:155–170.
65. Vega-Salas, D. E., P. J. I. Salas, D. Gundersen, and E. Rodriguez-Boulan. 1987. Formation of the apical pole of epithelial Madin-Darby canine kidney cells: polarity of an apical protein is independent of tight junctions while segregation of a basolateral marker requires cell–cell interactions. *J. Cell Biol.* 104:905–916.
66. Vega-Salas, D. E., P. J. I. Salas, and E. Rodriguez-Boulan. 1987. Modulation of the expression of an apical plasma membrane protein of Madin-Darby canine kidney epithelial cells: cell–cell interactions control the appearance of a novel intracellular storage compartment. *J. Cell Biol.* 104: 1249–1259.
67. Vestweber, D., R. Kemler, and P. Ekblom. 1985. Cell adhesion molecule uvomorulin during kidney development. *Dev. Biol.* 112:213–221.